Selective excitation study of Yb^{3+} in $GdCa_4O(BO_3)_3$ and $YCa_4O(BO_3)_3$

Selective excitation study of Yb³⁺ in GdCa₄O(BO₃)₃ and YCa₄O(BO₃)₃

A Lupei[1], G Aka[2], E Antic-Fidancev[2], B Viana[2], D Vivien[2] and P Aschehoug[2]

[1] Institute of Atomic Physics, Bucharest, MG 76900, Romania
[2] Laboratoire de Chimie Appliquée de l'Etat Solide, CNRS UMR 7574, ENSCP, 11, rue Pierre et Marie Curie F-75231 Paris, France

Abstract
The Yb³⁺-doped non-linear rare-earth calcium oxoborate crystals GdCa₄O (BO₃)₃ (GdCOB) and YCa₄O(BO₃)₃ (YCOB) were investigated by low-temperature absorption and selective excitation spectroscopy. The selective excitation and emission spectra revealed the spectral features of the main Yb³⁺ centre and the principal minority one in both crystals. The energy level schemes for these centres in both hosts, as well as structural assignments, were proposed. It was established that the minority centre, which represents about 10% of the total intensity and was assigned to Yb³⁺ in a Ca²⁺ site, is not a trap but an energy donor for the main centre. Common features of and differences between the vibronic structure of the two centres in GdCOB and YCOB are discussed. The existence of additional features in YCOB:Yb spectra is pointed out.

1. Introduction

Ytterbium-doped materials have been intensively studied during the last few years due to their potential use in diode-pumped solid-state lasers [1]. The main advantages of Yb³⁺ as a laser ion are the following: a simple electronic structure that excludes losses by cross relaxation; up-conversion or excited-state absorption; long radiative lifetimes; rather high quantum efficiency; low quantum defects. The fairly broad Yb³⁺ absorption and emission bands allow an efficient diode pumping and generation of tunable emission and short laser pulses. On the other hand, the main disadvantage of Yb³⁺ is that it works in a quasi-three-level configuration, and a large ground-state splitting is desirable.

The optical spectra of Yb³⁺(4f¹³) ions are complex owing to a strong electron–phonon coupling that leads to intense vibronic sidebands and additional effects such as shifting or splitting of lines in the case of resonant coupling [2–4]. Up to now, no reliable theoretical explanation of strong Yb³⁺ electron–phonon coupling in crystals has been given. An extension of the ideas of dynamic coupling effects [5] in the estimation of vibronic intensities for Yb³⁺

could be of real help. In many spectral studies on Yb^{3+} ions, one of the main problems is the identification of electronic Stark levels. For this purpose several methods have been used: first-principles crystal-field calculations; crystal-field calculations by using the available parameters for the various rare-earth (RE) ions in the same host and extrapolation of the results to Yb^{3+} ions [6]; a comparison of absorption and emission with lattice phonons; cooperative absorption [7]; use of the barycentres curve [8]. The relationship between the maximum crystal-field splitting of the $^2F_{7/2}$ Yb^{3+} ground manifold and that of $^4I_{9/2}$ of Nd^{3+} in the same matrix, deduced recently [9], could help to distinguish the highest Stark level of the $^2F_{7/2}$ manifold from vibronic sidebands. None of these methods give, however, an unambiguous answer as regards the assignment of Stark levels for Yb^{3+} ions.

Promising new laser materials with high potential for the 1 μm range as well as for green emission by self-frequency doubling include the non-linear RE and calcium oxoborates $RECa_4O(BO_3)_3$—RECOB crystals, especially those with $RE^{3+} = Y^{3+}$ or Gd^{3+}, doped with Yb^{3+} [10–19]. These crystals are non-hygroscopic and show high damage thresholds. Large crystals of good optical quality can be grown by the Czochralski method. Yb^{3+} can be introduced in these crystals in large concentrations without degradation of the crystal quality and the $^2F_{7/2}$ ground-manifold crystal-field splittings are rather large (of the order of 1000 cm^{-1}). RECOB crystals have a monoclinic structure, with space group *Cm*. The RECOB structure contains a unique RE site of C_s symmetry, two types of calcium site $Ca^{2+}(1)$ and $Ca^{2+}(2)$, and two distinct $(BO_3)^{3-}$ groups [20,21]. The RE^{3+} ion is coordinated by six close oxygen ions, two B^{3+} ions, and two O^{2-} at larger distances than the borons. Two oxygen ions nearest to the RE^{3+} cation, labelled O(1), do not belong to the borate groups, while the other six oxygen ions are members of these groups. The Ca^{2+} occupy two sites of C_1 symmetry: $Ca^{2+}(1)$ in a sixfold O^{2-} coordination; and $Ca^{2+}(2)$ in a distorted eightfold O^{2-} coordination and with two B^{3+} ions intercalated between the first six O^{2-} and the other two. Yb^{3+} ions can occupy the RE^{3+} sites of C_s symmetry, but also Ca^{2+} sites with a charge-compensation mechanism. A certain degree of disorder in the occupancy of RE or Ca^{2+} sites has already been reported in these crystals [10, 20, 21], but this problem still requires further investigations. Additional information on the dependence of this disorder on the host RE ion (Gd^{3+} or Y^{3+}) and on the dopant ion and its concentration could be obtained by low-temperature optical spectroscopy.

For a complete analysis of electron–phonon coupling effects, the phonon density of states is necessary, but in the absence of these density calculations, partial information can be obtained from Raman or IR spectra. In GdCOB crystals, all phonons are IR and Raman active and the spectra contain many sharp peaks at energies ranging from 48 to 1400 cm^{-1}. In the case of GdCOB, vibrational assignments have been proposed [22, 23], but the attributions of many phonon peaks are divergent. The phonon density of states for YCOB is expected to be similar to that of GdCOB, but only the main modes observed in Raman spectra were reported [24]. The optical spectra of Yb^{3+} in GdCOB and YCOB at room temperature have revealed more lines than expected for C_s or lower symmetries and were connected to electron–phonon coupling effects. Moreover, the low-temperature absorption and non-selectively excited emission on Yb^{3+} in GdCOB have shown the presence of a main and two minority centres [10]. The assignments of Stark electronic levels for main Yb^{3+} centres, made by different authors for GdCOB [10, 23] or YCOB [15, 25], are divergent, this attribution being complicated by the presence of non-equivalent centres.

This paper presents the results of the low-temperature absorption, selective excitation, and emission spectra for Yb^{3+} in GdCOB and YCOB hosts. The optical data allow us to underline differences between the two crystals by studying the spectral characteristics of non-equivalent centres. A discussion on the origin of these centres and their role in emission is presented. New assignments of the Stark electronic levels for the two Yb^{3+} centres in both crystals are proposed.

The attribution is mainly based on comparison of selective excitation and emission spectra, and with the known lattice phonon energies reported in the literature. Some characteristics of the electron–phonon coupling are also discussed.

2. Experiment

Good quality GdCOB:Yb and YCOB:Yb crystals grown by the Czochralski method in an iridium crucible under a nitrogen atmosphere with Yb^{3+} content from 5–15 at.% were investigated. The absorption spectra were recorded at 10 K for different polarizations by using a Cary 5 Varian spectrophotometer. The emission spectra as well as selective excitations were obtained with a CW Ti:sapphire laser (Coherent 890) pumped with an argon-ion laser. The spectra were analysed with an ARC SpectraPro-7510 monochromator and detected with a cooled InGaAs photodiode. The decay curves were recorded using a pulsed (10 ns) Ti:sapphire laser (BMI TS 802) pumped by a frequency-doubled YAG:Nd laser (BMI 501 DNS 720), a HD 460 Jobin–Yvon monochromator, and an InAs photodiode (1 μs time constant).

3. Experimental results

3.1. Low-temperature spectra of Yb^{3+} in GdCOB

3.1.1. Absorption and excitation spectra. The absorption spectra of Yb^{3+} in GdCOB with various concentrations ranging from 5 to 15 at.% were measured at 10 K for different polarizations. The samples were cut parallel to the optical axes (X, Y, Z) which are related to the crystallographic ones (a, b, c) as $b \parallel Y$, $(a, Z) = 26°$, $(c, X) = 15°$ for GdCOB and $b \parallel Y$, $(a, Z) = 24.7°$, $(c, X) = 13.5°$ for YCOB. The absorption spectrum of a 5 at.% Yb:GdCOB sample with $E \parallel X$ is presented in figure 1(a)) and shows three complex regions instead of only three lines that should be expected at low temperature (10 K) for $^2F_{7/2} \rightarrow {}^2F_{5/2}$ transition in a local symmetry of C$_s$ or lower. In the range A, corresponding to $^2F_{7/2}(1) \rightarrow {}^2F_{5/2}(1)$ transition (1 denoting the lowest Stark level of the manifold), a structure that was connected to non-equivalent sites [10] is observed. It has three components of Gauss shape that correspond to three Yb^{3+} centres: a main centre Yb$_1$ and two minority centres Yb$_2$ and Yb$_3$. The Yb$_2$ line (energy peaking at +16 cm^{-1} from Yb$_1$ at 10 245 cm^{-1}) has an intensity relative to the total spectrum of about $\sim$10% and this proportion is independent of the Yb^{3+} content, while for Yb$_3$ (energy peaking at $\sim$−10 cm^{-1} from Yb$_1$) the relative intensity is only 3%. The linewidths at half-intensity (FWHM) for the main centre increase from 7.5 cm^{-1} for 5 at.% to 9.5 cm^{-1} for 15 at.% Yb.

The absorption spectra in regions B and C (figure 1(a)) are a complex mixture of electronic lines for all non-equivalent centres and vibronic sidebands. The lines associated with a given centre could be separated by selective excitation. We were able to separate clearly the emission of two centres, Yb$_1$ and Yb$_2$. The excitation spectra of Yb$_1$ and Yb$_2$ centre emissions with polarization of excitation light $E \parallel X$ shown in figures 1(b) and (c) were measured by monitoring 976.1 nm 10 245 cm^{-1} (Yb$_1$) and 974.5 nm −10 261 cm^{-1} (Yb$_2$) emissions, respectively. The energy scale origin for the excitation spectra of Yb$_1$ and Yb$_2$ centres is taken at the lowest-energy absorption line for each centre. Such zero-lines could be affected by reabsorption and they are not presented in figures 1(b), (c). The intensity scales for excitation spectra are arbitrary. The excitation spectrum for the Yb$_1$ centre (figure 1(b)) looks like the absorption spectrum (figure 1(a)), unlike that for the Yb$_2$ centre (figure 1(c)). However, in each case the vibronic lines are rather strong and the assignment of 'pure' electronic lines in region B (figure 1) needs further analysis.
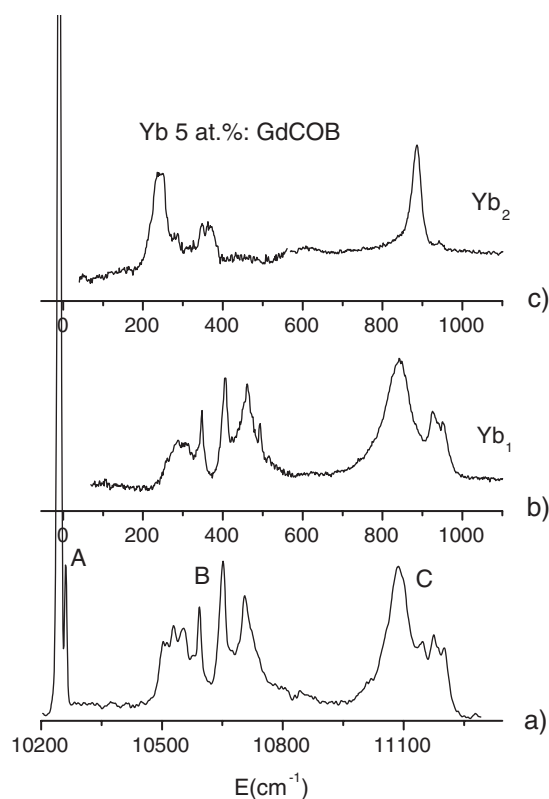
Figure 1. Yb^{3+} (5 at.% Yb^{3+}) in GdCOB at 10 K: (a) the absorption spectrum corresponding to $^2F_{7/2} \rightarrow {}^2F_{5/2}$ transition; (b) the excitation spectrum of Yb_1; and (c) the excitation spectrum of Yb_2 centres, shifted in energy relative to the zero-phonon lines.

3.1.2. Selectively excited emission spectra. The emission spectra at 10 K for a GdCOB sample with 5 at.% Yb^{3+} under selective excitation of Yb_1 (976.1 nm) and Yb_2 (974.5 nm) centres with $E \parallel X$ are presented in figure 2. Since the excitation was done at the zero-line $^2F_{7/2}(1) \rightarrow {}^2F_{5/2}(1)$ transition of the two centres, they are not shown in figure 2. These spectra should present at 10 K only three electronic lines corresponding to $^2F_{5/2}(1) \rightarrow {}^2F_{7/2}(2, 3, 4)$ transitions. One can observe a more complex structure in both spectra. Several lines in the emission spectra (figure 2(b)) are common to both excitations. For samples with larger Yb^{3+} content (15 at.%), the emission is practically independent of the excitation wavelength and the spectra are very similar. This suggests an energy transfer from Yb_2 to Yb_1 centres and was checked by the analysis of the emission decay profiles under excitation of Yb_2 centres in samples with low Yb^{3+} content (such as 5 at.% Yb^{3+}). For excitation with 974.5 nm (Yb_2), the decay of the Yb_2 centre emission is exponential with a lifetime of 2.5 ms (the continuous line in figure 3), while for the lines relating to the Yb_1 centre, the decays present a rise time (the dotted curve in figure 3). This energy transfer increases with temperature.

3.2. Spectra of Yb^{3+} in YCOB

Though the absorption and emission spectra of Yb^{3+} in YCOB have similarities to those obtained for GdCOB, some noticeable differences were observed. Besides the lines
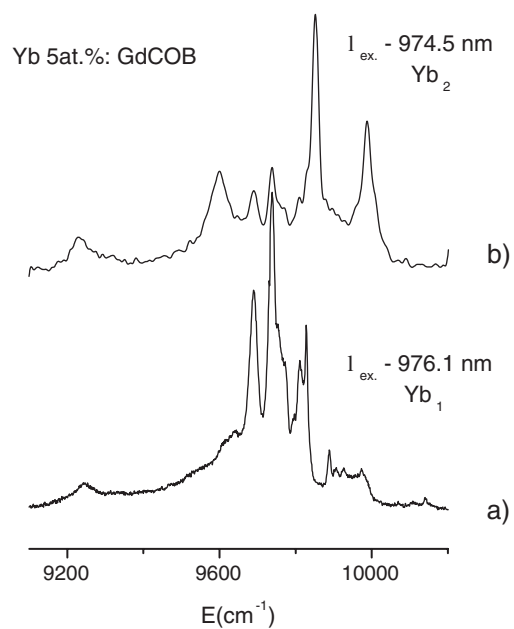
Yb 5at.%: GdCOB

l$_{ex.}$ - 974.5 nm
Yb$_2$

b)

l$_{ex.}$ - 976.1 nm
Yb$_1$

a)

9200   9600   10000

E(cm^{-1})

Figure 2. Emission spectra of two Yb^{3+} centres in GdCOB at 10 K under selective excitation at 976.1 nm (Yb$_1$) and 974.5 nm (Yb$_2$).

l$_{ex.}$ - 974.5nm

Yb$_2$

Yb$_1$

1.00

0.75

0.50

0.25

0.00

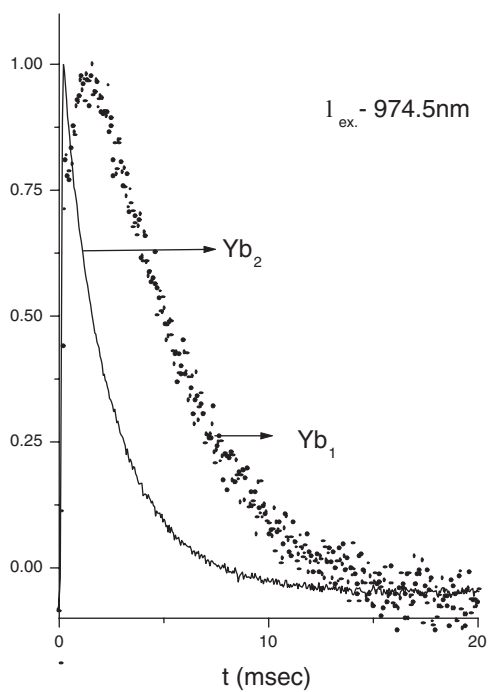0   10   20

t (msec)

Figure 3. Emission decay profiles of Yb$_2$ (continuous curve) and Yb$_1$ centres under excitation at 974.5 nm (Yb$_2$ centre).
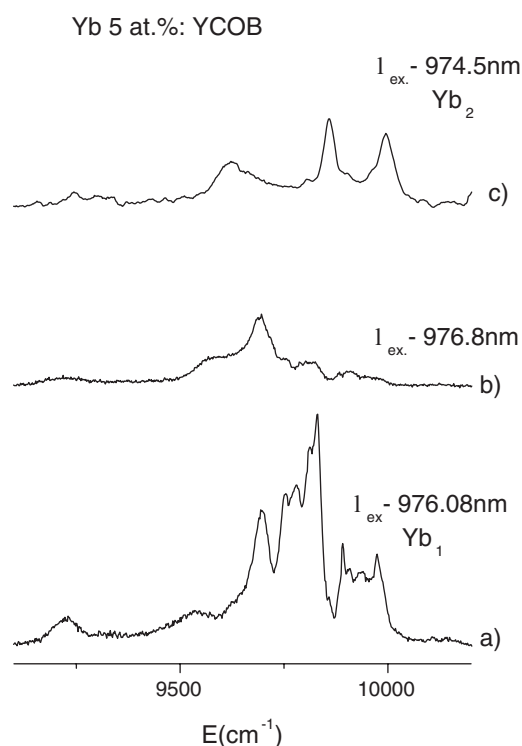
Figure 4. Emission spectra at 10 K for Yb^{3+} in YCOB at different excitation wavelengths: (a) 976.08 nm (Yb_1 centre), (b) 976.8 nm, and (c) 974.5 nm (Yb_2 centre).

corresponding to Yb_1 and Yb_2 centres, close to the main Yb^{3+} lines there is another rather intense component for the YCOB:Yb that is more difficult to separate by selective excitation, especially at high Yb^{3+} content. This is illustrated in figure 4 where the emission spectra for a 5 at.% Yb:YCOB sample, at three excitation wavelengths, are presented. While the emission spectra in figures 4(a) and (c) are similar to those observed for the two Yb_1 and Yb_2 centres in GdCOB, the emission under excitation at 976.8 nm (figure 4(b)) is clearly different and could not be related to the previous species. The same difference is observed in the excitation spectra in figure 5. Reabsorption effects were observed in the resonant transitions and this could affect the $^2F_{7/2}(1) \rightarrow {}^2F_{5/2}(3)$ transitions in excitation spectra (see figure 5(a) at the higher energy of about 11 100 cm^{-1}). Indeed, these emission and excitation spectra are different for Yb^{3+} ions in the two crystals, as suggested from the absorption spectra. As in the case of Yb:GdCOB, an energy transfer occurs between the minority Yb_2 centre and the main Yb_1 centre. The emission spectrum for large concentrations is independent of the excitation wavelength and is similar to that for Yb_1.

4. Discussion and conclusions

The results obtained from low-temperature absorption and selective excitation on Yb^{3+} in GdCOB and YCOB are discussed from two points of view: structural information and electron–phonon coupling.
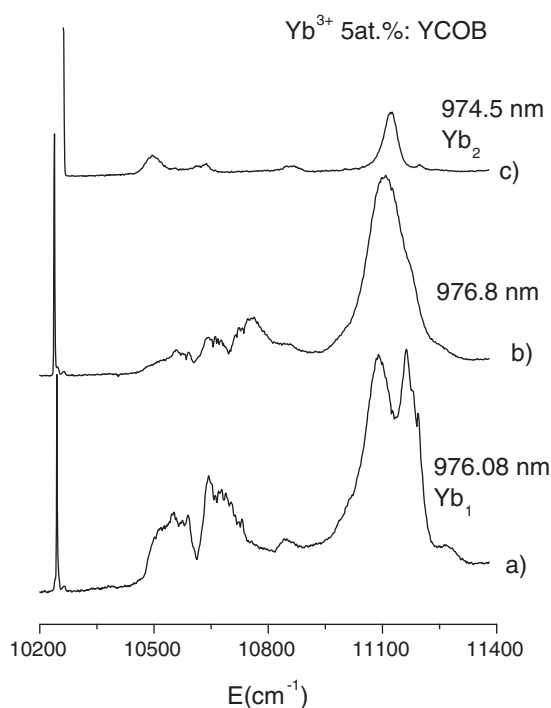
Figure 5. Excitation spectra at 10 K for different Yb^{3+} centres in YCOB: (a) 976.08 nm, (b) 976.8 nm, and (c) 974.5 nm.

4.1. Non-equivalent Yb^{3+} centres in GdCOB and YCOB

The low-temperature absorption, selective excitation, and emission spectra of Yb^{3+} in GdCOB and YCOB reveal the presence of a prevailing centre (Yb$_1$) and a less intense one (Yb$_2$), the relative intensity of the absorption for the two centres (about 10%) being practically independent of the Yb^{3+} content up to 15 at.%. Spectra of Yb^{3+} in YCOB are more complex than those of GdCOB:Yb; the former present at least one additional important component near the main Yb^{3+} centre. For both materials, the prevailing Yb$_1$ centres should correspond to Yb^{3+} in a Gd^{3+} or Y^{3+} site of C$_s$ symmetry, as proposed previously [10, 14]. The excitation and emission spectra of Yb$_2$ centres in both crystals suggest that this centre is connected to a different local surrounding for the Yb^{3+} ions. The Yb^{3+} ion could be located in a Ca^{2+} site, most likely Ca^{2+}(2) with a charge compensation. Arguments for this replacement are provided by the preference of RE^{3+} ions for eightfold rather than sixfold coordination and the similarities of the near neighbourhoods of the RE^{3+} and Ca^{2+}(2) sites [21]. The present study demonstrated that there is an energy transfer from the Yb$_2$ minority centre to the main Yb$_1$ centre; therefore Yb$_2$ centres are not energy traps for main-centre emission, though the minority Yb$_2$ centre represents around 10% of the total concentration. A similar centre was observed in Nd^{3+} spectra, but its relative concentration has been estimated to represent about 3% of the total concentration [27]. In the first published papers on the RECOB structure [20], the existence of some disorder in the occupancy of RE^{3+} and Ca^{2+} sites was suggested. It has been reported [20] that in pure RE^{3+} oxoborate crystals this disorder is minimum when the RE^{3+} ionic radius is close to that of Ca^{2+}, and is higher when this difference is higher, as is the case for Y^{3+}. This could also be a possible explanation for the difference between Nd^{3+}-

and Yb^{3+}-doped GdCOB and YCOB as regards the relative concentrations of Yb_2 centres. At the present time it is difficult to elucidate the nature of other structures observed in spectra of Yb^{3+} in YCOB. However, one should mention that differences between spectra of Nd^{3+} in GdCOB and YCOB have also been observed [27]—such as much larger linewidths in YCOB and different satellite structures in some transitions, and therefore a greater degree of disorder in the latter crystal. The presence of two main peaks in the differential thermal analysis (DTA) cooling curve [28] for YCOB (with only one for GdCOB) can be taken as an indication of a non-congruent melting behaviour that can be related to this disorder, but other studies aiming to explain the differences between the two crystals are in progress.

The $^2F_{7/2}(1) \rightarrow {}^2F_{5/2}(1)$ Yb^{3+} absorption lines at low temperature in GdCOB have Gauss shape and the widths of the main-centre zero-phonon lines increase slightly with Yb^{3+} content. This inhomogeneous broadening can be associated with the disorder and defects in these crystals. This behaviour can be linked to charged point defects determined by crystal non-stoichiometry or site inversions (for instance of the type $RE^{3+} \leftrightarrow Ca^{2+}$ [10, 20, 21]), or could correspond to calcium sites partially occupied by Yb^{3+}, as well as vacancies. Such charged point defects usually produce local random electric fields [26] and therefore shifts in the Yb^{3+} energy levels caused by the Stark effect, leading to inhomogeneous broadening. The widths are larger for Yb^{3+} in YCOB, due to the presence of at least one other component.

4.2. Electron–phonon coupling effects

The information on phonon energies in GdCOB and YCOB was obtained from Raman and IR data. In [22, 23] the internal vibrations for $(BO_3)^{3-}$ groups were found in the 590–1350 cm^{-1} domain, with strong lines in the Raman spectra at 933, 944, and at 739, 755 cm^{-1} in the IR spectrum. In [22] internal vibrations corresponding to Gd_xO_y or $Ca_\alpha O_\beta$ groups have been connected to peaks in the 376–508 cm^{-1} range, while the phonons in the 48–408 cm^{-1} range have been assigned to external modes of these groups. The electron–phonon coupling in these crystals exhibits strong vibronic bands observed in the Yb^{3+} spectra, which makes the assignment of Stark electronic levels difficult.

An attempt to use the selective excitation and emission data to determine the Stark level distribution for the two non-equivalent centres in the two crystals has been made. These data are especially useful as regards the minority centre Yb_2. For this purpose, the excitation and emission spectra for every centre—normalized to the $^2F_{7/2}(1) \leftrightarrow {}^2F_{5/2}(1)$ zero-phonon lines—were compared, as illustrated in figure 6 for the Yb_1 centre in GdCOB. The common lines in the two spectra seem to correspond to vibronic transitions. Thus, similar structure up to $\sim$408 cm^{-1} is observed in both spectra, and these lines are most probably vibronic ones. The lines marked by asterisks in the emission spectrum (figure 6(b)), in contrast, appear to be arising from electronic transitions, since they are missing in the excitation spectrum and no phonons with energies around $\sim$427, 550, or 993 cm^{-1} were reported. While the third Stark level of the excited $^2F_{5/2}$ manifold is easily separated (figure 6(a)) from a vibronic line at 933 cm^{-1}, the second Stark level was tentatively assigned as being in the 460 cm^{-1} region, though a phonon with such energy was reported on the basis of Raman spectra [22]. The strong vibronic lines are marked in figure 6(a). The last peak in the excitation spectrum is a vibronic one connected to the second Stark level, rather than to the 944 cm^{-1} vibration of the $(BO_3)^{3-}$ group. On the basis of a similar analysis, the electronic levels for the Yb_1 centre in YCOB were assigned as detailed in table 1. While the highest Stark levels (within experimental errors) for $^2F_{5/2}$ and $^2F_{7/2}$ are similar to previous assignments [10, 18, 23] (table 1), some differences appear for the intermediate ones.
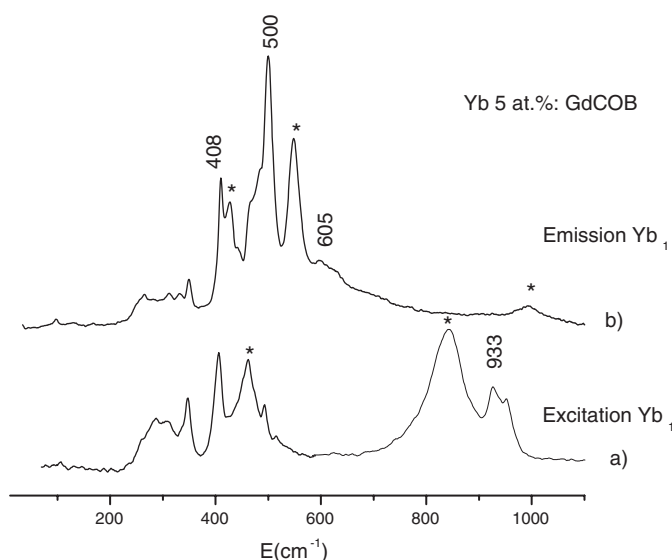
Figure 6. Selective excitation and emission spectra for the Yb_1 centre in GdCOB at 10 K. The spectra have as their origin the $^2F_{5/2}(1) \rightarrow {}^2F_{7/2}(1)$ lines, not presented in the figures. Asterisks denote the proposed Stark electronic levels and the main vibronic lines are marked.

Table 1. The proposed Stark level structure for Yb³⁺ centres in GdCOB and YCOB as compared with previous assignments.

	GdCOB				YCOB		
	Yb_1 (cm⁻¹)			Yb_2 (cm⁻¹)	Yb_1 (cm⁻¹)		Yb_2 (cm⁻¹)
Manifold	This work	Reference [10]	Reference [23]	This work	This work	Reference [18]	This work
$^2F_{7/2}$	0	0	0	0	0	0	0
	427	423	406	273	427	427	262
	550	668	547	660	550	556	639
	993	1 003	988	1 030	1 022	1 023	1 017
$^2F_{5/2}$	10 245	10 246	10 246	10 261	10 245	10 242	10 261
	10 706	10 706	10 706	10 630	10 676	10 537	10 632
	11 088	11 089	11 089	11 147	11 110	11 109	11 122

In the assignment of the electronic levels for the Yb_2 centre, the so-called barycentre curve approach was helpful [8]. According to the 'barycentre' approach, the plot of $^2F_{5/2}$ manifold barycentres versus $^2F_{7/2}$ ones, with the lowest Stark level as the origin, is a straight line for different crystals [8]. Indeed, for the free Yb³⁺ ions the separation of $^2F_{7/2}$ and $^2F_{5/2}$ manifolds is given by spin–orbit interaction. Since for Yb³⁺ ions embedded in a crystal the modifications of the spin–orbit coupling constant and the J-mixing are negligible, the separation of the two levels should be constant, independent of the matrix considered. If the Stark levels for one manifold are assigned, a barycentre curve can be used to derive the distribution of electronic lines for the other manifold. From the comparative analysis of the emission (figure 2(b)) and excitation spectra of the Yb_2 centre normalized at 10 261 cm⁻¹ (figure 1(c)), the most probable assignments of the electronic levels of $^2F_{7/2}$ are at 0, 273, 660, 1030 cm⁻¹. While the highest Stark level at 11 147 cm⁻¹ of the excited manifold $^2F_{5/2}$ is easily determined from the excitation

spectra of figure 1(c), phonons with energies corresponding to the excitation spectral lines at 245 and 350–370 cm^{-1}, reported also for Raman spectra [22], prevent the assignment of the second Stark level. The best fit to the barycentre curve (figure 1 in [8]) with the Yb$_2$ F$_{7/2}$ levels assigned above suggests the second electronic level, ^{2}F$_{5/2}$, at 10 630 cm^{-1}. A similar procedure was used for Yb$_2$ in YCOB, and all the attributions are gathered together in table 1.

One could use the data on Yb^{3+} centres and our recent results on Nd^{3+} in GdCOB and YCOB hosts [27] to check whether they satisfy well the relationship between the maximum splittings $\Delta E(^2\text{F}_{7/2})$ of Yb^{3+} and $\Delta E(^4\text{I}_{9/2})$ of Nd^{3+} manifolds [9]:

$$\Delta E(^2\text{F}_{7/2}) = 1.466 \, \Delta E(^4\text{I}_{9/2}).$$

In the case of Yb$_1$ centres, the estimated ratio of the maximum splittings is 1.48 for GdCOB, a value slightly closer to the theoretical one than the previous assignments [8], while the ratio is 1.5 for YCOB. For the minority Yb$_2$ centres, these ratios are 1.45 for GdCOB and 1.44 for YCOB. The data presented on Yb$_1$ and Yb$_2$ centres and their analogues for Nd^{3+} in GdCOB and YCOB are in good agreement.

The vibronic structures of Yb^{3+} in GdCOB and YCOB show some interesting features:

(i) In both crystals the spectra associated with the main Yb$_1$ centre present more vibronic lines than those for the Yb$_2$ centre (figures 1, 2, 4, 5). A possible explanation is the different structures of the two centres: while the Yb$_1$ centre has a strongly distorted eightfold O^{2-} coordination with two very close 'free' O(1) neighbours, Yb$_2$ corresponds most probably to a Ca^{2+}(2) site without such O(1) neighbours.

(ii) While the vibronic bands for Yb$_1$ in GdCOB and YCOB are similar in 260–450 cm^{-1} range, a noticeable difference is observed in the 450–520 cm^{-1} domain. A strong vibronic line corresponding to a phonon at $\sim$500 cm^{-1} is observed for GdCOB (figure 6), but is missing in the YCOB spectrum. Such a phonon line was observed in Raman spectra of GdCOB [22], but not reported among the main Raman modes in YCOB [24]. A strong vibronic band corresponding to a phonon energy of 500 cm^{-1} has been mentioned in the study of Gd^{3+} emission in GdCOB [29] and explained in terms of vibrations of GdO groups involving 'free' O(1) oxygens.

(iii) The spectra show a coupling with (BO$_3$)$^{3-}$ vibrations too—for instance, the coupling with a phonon at $\sim$933 cm^{-1} in absorption or excitation spectra of Yb$_1$ centres (figures 1(a), (b)) and with a phonon at 943 cm^{-1} in excitation spectra of Yb$_2$ centres (figure 1(c)). Vibronic lines with lower intensity could be associated with phonons of 600–640, 750 or 1250 cm^{-1} energies.

(iv) The electronic lines associated with ^{2}F$_{7/2}$(1) $\rightarrow$ ^{2}F$_{5/2}$(2, 3) transitions are broad due to electron–phonon effects. Thus, the Yb$_1$ main-centre line at 11 088 cm^{-1} in the absorption and excitation spectra for GdCOB (figures 1(a), (b)) has a Lorentz shape and a width of $\sim$70 cm^{-1}; this broadening is mainly due to the one-phonon near-resonant emission process, with emission of one phonon of energy $\sim$380 cm^{-1}. The second electronic line is also broadened by one-phonon emission ($\sim$460 cm^{-1}).

In conclusion, the low-temperature selective excitation and emission spectra of GdCOB:Yb^{3+} and YCOB:Yb^{3+}, obtained for the first time for a large variety of samples, show new aspects of the spectral characteristics and structural problems of these systems. The energy level schemes for two types of Yb^{3+} centre in both crystals are proposed. The experimental data suggest that the minority centre, which represents about 10% of the total intensity, could be assigned to Yb^{3+} in a Ca^{2+}(2) site. Energy transfer to the main centre occurs. The vibronic structures are different for two identified centres and some differences are also noticeable between the GdCOB:Yb and YCOB:Yb laser crystals. Some peculiarities observed in spectra of Yb^{3+} in YCOB suggest that this system requires further investigation.

Acknowledgments

References

[1]   DeLoach L D, Payne S A, Chase L L, Smith L K, Kway W L and Krupke W F 1993 *IEEE J. Quantum Electron.*
      29 1179
[2]   Perlin Yu E, Kaminskii A A, Enaki V N and Vileghanin D N 1979 *Pis. Zh. Eksp. Teor. Fiz.* **30** 426
[3]   DeLoach L D, Payne S A, Kway W L, Tassano J B, Dixit S N and Krupke W F 1994 *J. Lumin.* **62** 85
[4]   Lupei A, Lupei V, Presura C, Enaki V N and Petraru A 1999 *J. Phys.: Condens. Matter* **11** 376
[5]   Campos A F, Meijerink A, de Mello Donega C and Malta O L 2000 *J. Phys. Chem. Solids* **61** 1489
[6]   Chang N C, Gruber J B, Leavitt R P and Morrison C A 1982 *J. Chem. Phys.* **76** 3877
[7]   Peters V, Mix E, Peterman K, Huber G and Noginov M A 2000 *CLEO Europe, Technical Digest* p 387
[8]   Haumesser P H, Gaume R, Viana B, Antic-Fidancev E and Vivien D 2001 *J. Phys.: Condens. Matter* **13** 5427
[9]   Auzel F 2001 *J. Lumin.* **93** 129
[10] Mougel F, Dardenne K, Aka G, Kahn-Harari A and Vivien D 1997 *J. Opt. Soc. Am.* B **16** 164
[11] Chai B H, Hammons D A, Eichenholtz J, Ye Q, Jang W K, Shah L, Luntz G M, Richardson M and Qui H 1998
      OSA Topical Conf. on Advanced Solid State Lasers p 1147
[12] Jang W K, Eichenholtz J, Ye Q, Chai B H, Shah L, Peale R E, Richardson M and Qui H 1998 *Opt. Commun.*
      155 332
[13] Auge F, Balembois F, Georges P, Brun A, Mougel F, Aka G, Kahn-Harari A and Vivien D 1999 *Appl. Opt.* **38**
      976
[14] Zhang H, Meng X, Wang P, Zhu L, Liu X, Cheng R, Dawes J, Dekker P, Zhang S and Sun L 1999 *Appl. Phys.*
      B **8** 1147
[15] Aka G *et al* 2000 *J. Alloys Compounds* **303–4** 401
[16] Druon F, Auge F, Balembois F, Georges P, Brun A, Aron A, Mougel F, Aka G and Vivien D 2000 *J. Opt. Soc.*
      Am. B **17** 18
[17] Richardson M, Hammons D, Eichenholtz J, Chai B H T, Ye Quing, Jang Won Kweon and Shah L 2000 *J. Kor.*
      Phys. Soc. **37** 633
[18] Zhang H, Meng X, Zhu L, Wang P, Liu X, Dawes J, Dekker P, Cheng R, Zhang S and Sun L 2000 *Mater. Res.*
      Bull. **35** 799
[19] Zhang H, Meng X, Wang P, Zhu L, Liu X, Yang Y, Wang R, Dawes J, Piper J, Zhang S and Sun L 2001 *J. Cryst.*
      Growth **222** 209
[20] Ilyukhin B and Dzhurinskii B F 1993 *Russ. J. Inorg. Chem.* **38** 847
[21] Norrestam R, Nygren M and Bovin J O 1992 *Chem. Mater.* **4** 738
[22] Lorriaux-Rubbens A, Aka G, Antic-Fidancev E, Keszler D A and Wallart F 2000 *J. Raman Spectrosc.* **31** 535
[23] Dominiak-Dzik G, Ryba-Romanovski W, Golab S, Macalik L, Hanuza A and Pajaczkowska A 2000 *J. Mol.*
      Struct. **555** 213
[24] . Li X L, Guo M, Jiang H D, Hu X B, Shao Z S, Wang J Y, Wei J Q, Xia H R, Liu Y G and Jiang M H 2000
      Cryst. Res. Technol. **35** 11–12 1361
[25] Aron A *et al* 2001 *Opt. Mater.* **16** 181
[26] Stoneham M 1969 *Rev. Mod. Phys.* **41** 82
[27] Lupei A, Antic-Fidancev E, Aka G, Vivien D, Aschehoug P, Goldner Ph, Pellé F and Gheorghe L 2001 submitted
[28] Vivien D *et al* 2002 *J. Cryst. Growth* at press
[29] Dirksen G J and Blasse G 1993 *J. Alloys Compounds* **191** 121